

1 **REVISION 1**

2 **Bicapite,  $\text{KNa}_2\text{Mg}_2(\text{H}_2\text{PV}^{5+}_{14}\text{O}_{42})\cdot 25\text{H}_2\text{O}$ , a new polyoxometalate mineral with**  
3 **a bicapped Keggin anion from the Pickett Corral mine, Montrose County,**  
4 **Colorado, U.S.A.**

5  
6 **ANTHONY R. KAMPF<sup>1</sup>✉, JOHN M. HUGHES<sup>2</sup>, BARBARA P. NASH<sup>3</sup>, AND JOE MARTY<sup>4</sup>**

7  
8  
9 <sup>1</sup>Mineral Sciences Department, Natural History Museum of Los Angeles County, 900  
10 Exposition Boulevard, Los Angeles, California 90007, U.S.A.

11 <sup>2</sup>Department of Geology, University of Vermont, Burlington, VT 05405, U.S.A.

12 <sup>3</sup>Department of Geology and Geophysics, University of Utah, Salt Lake City, Utah 84112, U.S.A.

13 <sup>4</sup>5199 East Silver Oak Road, Salt Lake City, UT 84108, U.S.A.

14  
15  
16 **ABSTRACT**

17  
18 Bicapite,  $\text{KNa}_2\text{Mg}_2(\text{H}_2\text{PV}^{5+}_{14}\text{O}_{42})\cdot 25\text{H}_2\text{O}$ , is a new mineral species (IMA2018-048)

19 discovered at the Pickett Corral mine, Montrose County, Colorado. Bicapite occurs as square  
20 tablets up to about 0.2 mm on edge on montroseite-corvusite-bearing sandstone. Crystals are  
21 dark red-brown, often appearing black. The streak is orange and the luster is vitreous. Bicapite is  
22 brittle, has a Mohs hardness of 1½, and displays one excellent cleavage on {100}. The measured  
23 density is 2.44(2) g·cm<sup>-3</sup>. Bicapite is uniaxial (+),  $\omega = 1.785(5)$ ,  $\varepsilon \approx 1.81$  (white light);  
24 pleochroism is red-brown;  $E > O$ , slight. The electron probe microanalysis and results of the  
25 crystal structure determination provided the empirical formula (based on 67 O apfu)  
26  $(\text{K}_{1.23}\text{Na}_{2.23}\text{Mg}_{1.48})_{\Sigma 4.94}[\text{H}_{2.51}\text{P}_{1.02}(\text{V}^{5+}_{13.91}\text{Mo}^{6+}_{0.07})_{\Sigma 13.98}\text{O}_{42}]\cdot 25\text{H}_2\text{O}$ . Bicapite is tetragonal,  $I4/m$ ,  
27 with  $a = 11.5446(12)$ ,  $c = 20.5460(14)$  Å,  $V = 2738.3(6)$  Å<sup>3</sup>, and  $Z = 2$ . The strongest four lines  
28 in the diffraction pattern are [ $d$  in Å( $I$ )( $hkl$ ): 10.14(100)(002, 101), 2.978(29)(134, 206),  
29 2.809(11)(305), and 2.583(11)(420, 008). The atomic arrangement of bicapite was solved and

---

✉E-mail: [akampf@nhm.org](mailto:akampf@nhm.org)

30 refined to  $R_1 = 0.0465$  for 1008 independent reflections with  $I > 2\sigma I$ . The structural unit is a  
31  $[\text{H}_2\text{PV}^{5+}_{12}\text{O}_{40}(\text{V}^{5+}\text{O})_2]^{7-}$  heteropolyanion composed of twelve distorted  $\text{VO}_6$  octahedra  
32 surrounding a central  $\text{PO}_4$  tetrahedron and capped on opposite sides by two  $\text{VO}_5$  square  
33 pyramids; the structural unit is a modification of the  $\alpha$ -isomer of the Keggin anion,  $[\text{XM}_{12}\text{O}_{40}]^{n-}$ .  
34 Charge balance in the structure is maintained by the  $[\text{KNa}_2\text{Mg}_2(\text{H}_2\text{O})_{25}]^{7+}$  interstitial complex.  
35 The name bicapite is in recognition of this being the only known mineral with a structure based  
36 on a bicapped Keggin anion. The discovery of bicapite and numerous other natural  
37 polyoxometalate compounds in the Colorado Plateau uranium/vanadium deposits make that the  
38 most productive region found to date for naturally occurring polyoxometalate compounds.

39

40 **Keywords:** Bicapite; new mineral; crystal structure; polyoxometalate; bicapped Keggin  
41 anion; Pickett Corral mine, Montrose County, Colorado, USA

42

43  
44  
45  
46  
47  
48  
49  
50  
51  
52  
53  
54  
55  
56  
57  
58  
59  
60  
61  
62  
63  
64  
65

## INTRODUCTION AND OCCURRENCE

The arcuate 120 km-long Uravan Mineral Belt of the Colorado Plateau has been a rich source of uranium and vanadium ore since early in the twentieth century. The numerous mines in the belt exploit roll-front deposits in sandstone of the Salt Wash member of the Morrison Formation (Carter and Gultierri 1965; Shawe 2011). The mineralization of U and V took place where solutions rich in  $U^{6+}$ - and  $V^{4+}/V^{5+}$ -bearing aqueous species encountered local strongly reducing conditions, typically due to the presence of organic matter. The details of the geochemistry of the deposits and conditions of deposition were first examined in detail by Evans and Garrels (1958). The uranium and vanadium deposits of the Uravan Mineral Belt have also been a rich source of new minerals; more than 30 minerals with essential vanadium have been discovered there since 2008 during collecting undertaken by one of the authors (JM) and his colleagues. These minerals have added extensively to the knowledge of the complexity of naturally occurring vanadium compounds.

The new mineral bicapite was found underground in the Pickett Corral mine, Bull Canyon, Montrose County, Colorado, about 13 km west of the town of Naturita. The portal to the Pickett Corral mine is located at 38.195272, -108.843326; however, the partially flooded workings of the mine were accessed through the main portal of the interconnected Blue Streak mine located at 38.199434, -108.839946. The Pickett Corral mine is in the central portion of the Uravan Mineral Belt. The new mineral forms from the oxidation of montroseite-corvusite assemblages in a moist environment. Under ambient temperatures and generally oxidizing near-surface conditions, water reacts with pyrite to form aqueous solutions with relatively low pH; this water reacts with unoxidized and oxidized phases that have been exposed by mining operations to form bicapite and other new mineral species.

66 The name bicapite is in recognition of this being the only known mineral with a structure  
67 based on a bicapped Keggin anion. The mineral was collected on March 24, 2016, by one of the  
68 authors (JM), Al Wilkins and Okie Howell. It has been found very sparingly on only several  
69 small specimens. It occurs on montroseite-corvusite-bearing sandstone in close association with  
70 gypsum, huemulite, and thenardite. Bicapite was approved by the Commission on New Minerals,  
71 Nomenclature, and Classification of the International Mineralogical Association (IMA 2018–  
72 048). Two cotype specimens of bicapite are deposited in the collections of the Natural History  
73 Museum of Los Angeles County, Los Angeles, California, USA, catalogue numbers 66915 and  
74 66916.

#### 75 POLYOXOMETATES

76 Polyoxometalate compounds (often abbreviated as *POMs*) are relatively rare in geology,  
77 but of great importance in synthetic chemistry and materials science. Polyoxometalates, usually  
78 anionic in nature, are clusters of three or more transition metal-centered polyhedra that are linked  
79 by sharing oxygen ligands between and among the polyhedra. The linked polyhedra form a  
80 three-dimensional framework. One example of a polyoxometalate compound recently found to  
81 be common to numerous minerals in the Colorado Plateau deposits is the  $[V_{10}O_{28}]^{6-}$   
82 isopolyanion, the decavanadate group, formed of 10  $VO_6$  octahedra linked through corner- and  
83 edge-sharing. Typically, bonding within the polyoxometalate is stronger than between the  
84 polyoxometalate and the surrounding crystal field.

85 Polyoxometalates are important phases in industrial chemistry, where a large effort is  
86 expended in synthesizing polyoxometalates with desirable characteristics of size, charge, shape  
87 and conformation. Many hundreds of papers are published annually in the chemistry literature on  
88 polyoxometalates, and the number of papers has been increasing logarithmically since the early

89 1990s (Hutin et al. 2013); a similar increase in patents involving polyoxometalates is also noted  
90 (Katsoulis 1998). In a detailed survey of industrial uses of polyoxometalates, Katsoulis (1998)  
91 notes that 80-85% of the patents issued for polyoxometalates are in the area of catalysis, with the  
92 remaining 15-20% involving the compounds in nearly a score of other applications, including  
93 coatings, sorbents of gases, sensors, dyes, capacitors, cation exchangers, anti-tumor agents, and  
94 bleaching of pulp paper. New uses of polyoxometalate compounds have been in medicine as  
95 antiviral agents, cancer antagonists and treatment for Alzheimer's disease, and in  
96 nanomagnetism with applications to semiconductors and quantum computing.

97         There are many methods of synthesis of polyoxometalates, but the most common method  
98 is undertaken using acidic aqueous systems that contain the relevant polyoxometalate cations and  
99 the cations needed to balance the charge of the anionic polyoxometalate at a controlled pH;  
100 molybdate and tungstate polyoxometalates tend to occur at lower pH values than vanadate  
101 POMs. The conditions of vanadium polyoxometalate formation in laboratory aqueous synthesis  
102 are similar to the natural post-mining conditions found in the Colorado plateau vanadium-  
103 uranium mines, where solutions rich in vanadium for the POM formation as well as charge-  
104 balancing cations exist at a suitable pH.

105         Although polyoxometalate compounds are not common in minerals, they do exist, and a  
106 growing number of POMS are being discovered in the Colorado Plateau Uranium Belt; these  
107 phases are listed subsequently. In addition to those minerals with a similar Colorado Plateau  
108 genesis to bicapite, POM-bearing minerals include zunyite (Baur and Ohta 1982) and murataite  
109 (Ercit and Hawthorne 1995); however, in these minerals, the keggings-type polyoxometalates are  
110 condensed into frameworks and do not contain independent polyoxometalate units. The Colorado  
111 Plateau deposits have enlarged the number of POM-bearing minerals greatly, and that region is

112 the most productive region found to date for naturally occurring polyoxometalate compounds.

113 **APPEARANCE, OPTICAL AND PHYSICAL PROPERTIES**

114 Bicapite occurs as square tablets up to about 0.2 mm on edge (Figures 1 and 2); the  
115 crystals are dark red-brown, often appearing black. The streak is orange and the luster is vitreous.  
116 Bicapite is non-fluorescent under long- and short-wave ultraviolet light. It is brittle, has a Mohs  
117 hardness of 1½ (based upon scratch tests), and exhibits excellent cleavage on {100}; the fracture  
118 is irregular, stepped. The density measured by flotation in methylene iodide – toluene is 2.44(2)  
119 g·cm<sup>-3</sup>; the calculated density is 2.434 g·cm<sup>-3</sup> for the empirical formula and 2.428 g·cm<sup>-3</sup> for the  
120 ideal formula. Bicapite is very slowly soluble in room-temperature H<sub>2</sub>O (~1 hour); the phase  
121 decomposes in dilute HCl at room temperature and then slowly dissolves.

122 Optical observations on bicapite were made in white light. Bicapite is uniaxial (+), with  $\omega$   
123 = 1.785(5) and  $\epsilon \approx 1.81$ . Note that  $\epsilon$  is observed to be slightly greater than 1.80; in liquids > 1.80,  
124 crystals of an unknown phase immediately grow on the surfaces of the bicapite crystals.  
125 Pleochroism is red-brown;  $E > O$ , slight. The Gladstone-Dale compatibility (Mandarino 2007),  
126  $(1 - (K_p/K_c))$ , is -0.017, is (superior) using the empirical formula, and -0.019 (superior) using the  
127 ideal formula.

128

129 **CHEMICAL COMPOSITION**

130 Analyses of bicapite (4 points on 3 crystals) were performed at the University of Utah on  
131 a Cameca SX-50 electron microprobe with four wavelength dispersive spectrometers, and  
132 utilizing Probe for EPMA software. Analytical conditions were 15 keV accelerating voltage, 10  
133 nA beam current and a beam diameter of 5 to 10  $\mu$ m. Counting times were 20 seconds on peak  
134 and 20 seconds on background for each element. Raw X-ray intensities were corrected for matrix

135 effects with a  $\phi\rho(z)$  algorithm (Pouchou and Pichoir 1991). A time-dependent correction was  
136 applied to the data for Na to allow for an intensity decrease during analysis. All others elements  
137 exhibited no time-dependence in intensity.

138 No damage from the electron beam was observed. However, as is typical of highly  
139 hydrated phases with weakly held H<sub>2</sub>O, bicapite partially dehydrates under vacuum either during  
140 carbon coating or in the microprobe chamber. This results in an irregular surface for analysis. In  
141 addition, the H<sub>2</sub>O loss results in higher concentrations for the remaining constituents than are to  
142 be expected for the fully hydrated phase. Because an insufficient quantity of bicapite is available  
143 for a direct determination of H<sub>2</sub>O, that content has been calculated based upon the structure  
144 determination. Element concentrations are given in Table 1.

145 The empirical formula (based on 42 O apfu in structural unit) is  
146  $(K_{1.23}Na_{2.23}Mg_{1.48})_{\Sigma 4.94}[H_{2.51}P_{1.02}(V^{5+}_{13.91}Mo^{6+}_{0.07})_{\Sigma 13.98}O_{42}] \cdot 25H_2O$ . The simplified formula is  
147  $KNa_2Mg_2(H_2PV^{5+}_{14}O_{42}) \cdot 25H_2O$ , which corresponds to K<sub>2</sub>O 2.35, Na<sub>2</sub>O 3.10, MgO 4.03, P<sub>2</sub>O<sub>5</sub>  
148 3.54, V<sub>2</sub>O<sub>5</sub> 63.59, H<sub>2</sub>O 23.39, total 100 wt%.

149

## 150 CRYSTAL STRUCTURE EXPERIMENTAL

151 The X-ray powder diffraction study was performed using a Rigaku R-Axis Rapid II  
152 curved imaging plate microdiffractometer with monochromatized MoK $\alpha$  radiation. A Gandolfi-  
153 like motion on the  $\phi$  and  $\omega$  axes was used to randomize the samples. Observed  $d$  values and  
154 intensities were derived by profile fitting using JADE 2010 software. Data, including unit-cell  
155 parameters refined from the powder data using JADE 2010 with whole pattern fitting, are given  
156 in Table 2.

157 Single-crystal X-ray studies were carried out using the same instrument and radiation  
158 noted above. The Rigaku CrystalClear software package was used for processing the structure  
159 data, including the application of numerical and empirical absorption corrections, the latter with  
160 the multi-scan approach using ABSCOR (Higashi 2001). The structure was solved by direct  
161 methods using SIR2011 (Burla et al. 2012). SHELXL-2016 (Sheldrick 2015) was used for the  
162 refinement of the structure. The occupancies of the interstitial cation sites were refined, with the  
163 K site refined with full joint occupancy by K and O (H<sub>2</sub>O). A residual peak 2.229(17) Å from the  
164 K site was refined as an additional low-occupancy H<sub>2</sub>O site; however, based upon distances to  
165 surrounding O sites, it could also accommodate additional Na. All non-hydrogen sites were  
166 refined with anisotropic displacement parameters. Difference Fourier syntheses located all H  
167 atom positions, except those associated with the partially occupied H<sub>2</sub>O sites and those that  
168 protonate the bicapped Keggin anion. The H sites were refined with soft restraints of 0.82(3) Å  
169 on the O–H distances and 1.30(3) Å on the H–H distances; the  $U_{eq}$  of each H was set to 1.2 times  
170 that of the donor O atom. Data collection and refinement details are given in Table 3, atom  
171 coordinates and displacement parameters in Table 4, selected bond distances in Table 5 and  
172 bond-valence sums in Table 6.

173

#### 174 **ATOMIC ARRANGEMENT OF BICAPITE**

175 The atomic arrangement of bicapite (Figures 3 and 4) consists of two distinct parts, a  
176 structural unit and an interstitial complex, as suggested by Schindler and Hawthorne (2000) for  
177 such hydrated minerals with a polyanion. The structural unit is a  $[\text{H}_2\text{PV}^{5+}_{12}\text{O}_{40}(\text{V}^{5+}\text{O})_2]^{7-}$   
178 heteropolyanion composed of twelve distorted VO<sub>6</sub> octahedra surrounding a central PO<sub>4</sub>  
179 tetrahedron and capped on opposite sides by two VO<sub>5</sub> square pyramids, which share four of their



180 edges with VO<sub>6</sub> octahedra (Figure 3). Without the two capping tetrahedra (and H atoms of the  
181 structural unit), the heteropolyanion is the  $\alpha$ -isomer of the Keggin anion, [XM<sub>12</sub>O<sub>40</sub>]<sup>n-</sup>, which in  
182 this case has the formula [PV<sup>5+</sup><sub>12</sub>O<sub>40</sub>]<sup>15-</sup>. In light of the bond valence sum (BVS) values for the  
183 V sites all being slightly greater than 5 vu, all V in the mineral is likely to be in the +5 oxidation  
184 state. The central PO<sub>4</sub> tetrahedron is disordered, with eight half-occupied O atoms around the P.  
185 This is consistent with the P residing at the 0, 0, ½ special position with 4/m symmetry. Attempts  
186 to refine the structure in a space group that would allow P to occupy a site with -4 symmetry  
187 were unsuccessful. It should be noted that this same sort of averaged orientation of the central  
188 Keggin tetrahedron has been reported in other structures (cf. Nyman et al. 2007).

189 The interstitial complex includes two octahedrally coordinated cation sites, one occupied  
190 by Mg and surrounded by six H<sub>2</sub>O groups and one occupied by Na and surrounded by five H<sub>2</sub>O  
191 groups and one O atom. The Mg(H<sub>2</sub>O)<sub>6</sub> octahedron is isolated and only links to other structural  
192 components via hydrogen bonding. The NaO(H<sub>2</sub>O)<sub>5</sub> octahedra form dimers by linking through  
193 one shared H<sub>2</sub>O group. Each end of the dimer is an O atom shared with the apical O atoms of the  
194 VO<sub>5</sub> square pyramids that cap different bicapped Keggin anions. Above the four square  
195 “cavities” in each bicapped Keggin anion is the site jointly occupied by K and H<sub>2</sub>O. When the  
196 site is occupied by K, it forms bonds to the four O atoms at the corners of the cavity, one bond to  
197 an O atom in a different bicapped Keggin anion and three bonds to H<sub>2</sub>O groups belonging to the  
198 NaO(H<sub>2</sub>O)<sub>5</sub> octahedra. When the K site is occupied by the O atom of an H<sub>2</sub>O group, it  
199 presumably forms hydrogen bonds to surrounding O atoms. One such bond is probably to O4,  
200 thereby compensating for its otherwise low BVS (1.86 vu).

201 The interstitial complex ideally has the formula [KNa<sub>2</sub>Mg<sub>2</sub>(H<sub>2</sub>O)<sub>25</sub>]<sup>7+</sup>, which, for charge  
202 balance, requires that the structural unit is doubly protonated. Although no specific H sites could

203 be identified on the periphery of the bicapped Keggin anion, among synthetic bicapped Keggin  
204 anions, protonation is quite common. For example, Kato et al. (1982) described a similar  
205 bicapped Keggin anion for which they gave the formula  $H_nPV_{14}O_{42}^{(9-n)-}$ . In bicapite, the most  
206 likely candidate O sites for partial OH character are probably O2, O3 and O4, because of their  
207 somewhat low BVS values and their locations on the periphery of the structural unit, although as  
208 noted above, the low BVS for O4 may be compensated by a hydrogen bond from the H<sub>2</sub>O group  
209 partially occupying the K site. The low BVS for the PO<sub>4</sub> group O1 site (1.69 vu) is probably due  
210 to steric effects rather than being indicative of partial OH character. For comparison, the O atom  
211 of the PO<sub>4</sub> group in the similar bicapped Keggin anion reported by Kato et al. (1982) is 1.74 vu  
212 corresponding to a P–O bond length of 1.529 Å (identical to the P–O distance in bicapite).

213 A note on bonding within the structural unit and between the structural unit and the  
214 interstitial complex is in order. The exterior oxygen atoms of the heteropolyanionic structural  
215 unit that protrude into the interstitial unit (O2, O3, O4), known as “terminal” oxygens, are all  
216 bound to the vanadium atoms of the structural unit by vanadyl bonds (Table 5; Schindler et al.  
217 2000), as is a fourth oxygen atom (O7) that is also an exterior atom but not a terminal oxygen.  
218 Three of these four oxygen atoms are shared with atoms of the interstitial complex (Na-O2, K-  
219 O4, K-O7). In addition, O6, although not bonded to vanadium with a vanadyl bond, is bound to  
220 two vanadium atoms in addition to the interstitial, partially occupied, K site. The strongly  
221 anisodesmic nature of bonding in the polyanionic structural group is illustrated by the bond  
222 valence (in valence units, *vu*) each of its oxygen atoms receives from the cations of the  
223 polyanion: O1 = 1.69; O2 = 1.68; O3 = 1.69; O4 = 1.81; O5 = 1.98; O6 = 1.84; O7 = 1.88). Such  
224 bonding has implications for the solution behavior of the polyanions and ion transport in the ore-  
225 forming fluids of the Colorado Plateau.

226  
227

## IMPLICATIONS

228 Over the past several years, numerous new minerals have been described from the mines  
229 of the Colorado Plateau. In addition to the previously described Colorado Plateau mineral  
230 sherwoodite (Evans and Konnert 1978) and numerous new  $[\text{V}_{10}\text{O}_{28}]^{6-}$  decavanadate minerals  
231 (Kampf et al. 2017a), there is a growing number of recently described Colorado-Plateau minerals  
232 with large, complex heteropolyanions. The minerals vanarsite, packratite, morrisonite and  
233 gatewayite all contain the  $[\text{As}^{3+}\text{As}^{5+}_6\text{V}^{4+}_{2+x}\text{V}^{5+}_{10-x}\text{O}_{51}]^{(11+x)-}$  heteropolyanion, a novel  
234 polyoxometalate cluster (Kampf et al. 2016). The mineral kegginite (Kampf et al. 2017b)  
235 contains the  $[\text{As}^{5+}\text{V}^{5+}_{12}\text{O}_{40}(\text{VO})]^{12-}$  monocapped  $\epsilon$ -isomer of the Keggin heteropolyanion, and  
236 ophirite contains a heteropolytungstate tri-lacunary Keggin anion  $[\text{Fe}^{3+}\text{W}_9\text{O}_{34}]_2^{11-}$  (Kampf et al.  
237 2014). Herein we describe bicapite, a mineral whose structure contains the  
238  $[\text{H}_2\text{PV}^{5+}_{12}\text{O}_{40}(\text{V}^{5+}\text{O})_2]^{7-}$  protonated bicapped  $\alpha$ -isomer of the Keggin heteropolyanion. Other new  
239 minerals of the region that contain large heteropolyions, both anionic and cationic, are currently  
240 under study. The mines of the Colorado Plateau are a rich source of minerals with complex  
241 heteropolyions that have formed in low-temperature, post-mining mineral assemblages,  
242 apparently similar to the “one-pot” bench-scale synthesis of polyoxometalates in inorganic  
243 chemistry (Hutin et al. 2013), and obviously forming in a self-assembling environment. The  
244 discovery and study of those self-organizing nanostructures advance our knowledge and  
245 understanding of mineral complexity on Earth, provide new insights into complex ions that can  
246 exist in near-surface environments, and inform researchers in other fields of new avenues to  
247 explore in developing phases with potential technological uses. The Colorado Plateau  
248 uranium/vanadium deposits encompass the most productive region found to date for naturally  
249 occurring polyoxometalate compounds.

250

251

### **ACKNOWLEDGMENTS**

252

The manuscript was improved by reviews by Michael Schindler and an anonymous

253

review. Editorial handling by Fernando Colombo is greatly appreciated. This study was funded,

254

in part, by the John Jago Trelawney Endowment to the Mineral Sciences Department of the

255

Natural History Museum of Los Angeles County and by grant NSF-MRI 1039436 from the

256

National Science Foundation to JMH. BPN thanks the Northern California Mineralogical

257

Association for partial support for electron microprobe analyses of new minerals from the

258

Colorado Plateau.

259

## REFERENCES

- 260 Baur, W.H., and Ohta, T. (1982) The  $\text{Si}_5\text{O}_{16}$  pentamer in zunyite refined and empirical relations  
261 for individual silicon-oxygen bonds. *Acta Crystallographica*, B38, 390-401.
- 262 Burla, M.C., Caliandro, R., Camalli, M., Carrozzini, B., Cascarano, G. L., De Caro, L.,  
263 Giacobozzo, C., Polidori, G., and Spagna, R. (2005) SIR2004: an improved tool for crystal  
264 structure determination and refinement. *Journal of Applied Crystallography*, 38, 381-388.
- 265 Carter, W.D. and Gualtieri, J.L. (1965) Geology and uranium–vanadium deposits of the La Sal  
266 quadrangle, San Juan County, Utah, and Montrose County, Colorado. United States  
267 Geological Survey Professional Paper 508.
- 268 Ercit, T.S., and Hawthorne, F.C. (1995) Murataite, a  $\text{UB}_{12}$  derivative structure with condensed  
269 Keggin molecules. *Canadian Mineralogist*, 33, 1223-1229.
- 270 Evans, H.T., Jr., and Garrels, R.M. (1958) Thermodynamic equilibria of vanadium in aqueous  
271 systems as applied to the interpretation of the Colorado Plateau ore deposits. *Geochimica et*  
272 *Cosmochimica Acta*, 15, 131-149.
- 273 Evans, Jr., H.T., Jr., and Konnert, J.A. (1978) The crystal chemistry of sherwoodite, a calcium  
274 14-vanadoaluminate heteropoly complex. *American Mineralogist*, 63, 863–868.
- 275 Ferraris, G. and Ivaldi, G. (1988) Bond valence vs. bond length in O...O hydrogen bonds. *Acta*  
276 *Crystallographica*, B44, 341–344.
- 277 Gagné, O.C. and Hawthorne, F.C (2015) Comprehensive derivation of bond-valence parameters  
278 for ion pairs involving oxygen. *Acta Crystallographica*, B71, 562–578.
- 279 Higashi, T. (2001) *ABSCOR*. Rigaku Corporation, Tokyo.
- 280 Hutin, M., Rosnes, M.H., Long, D.-L., and Cronin, L. (2013) Polyoxometalates: Synthesis and  
281 structure – From building blocks to emergent structures. *In*: Jan Reedijk and Kenneth

- 282 Poeppelmeier, editors. Comprehensive Inorganic Chemistry II, Vol 2. Oxford: Elsevier,  
283 2013, p. 241-269.
- 284 Kampf, A.R., Hughes, J.M., Nash, B.P., Wright, S.E., Rossman, G.R., and Marty, J. (2014)  
285 Ophirite,  $\text{Ca}_2\text{Mg}_4[\text{Zn}_2\text{Mn}^{3+}_2(\text{H}_2\text{O})_2(\text{Fe}^{3+}\text{W}_9\text{O}_{34})_2]\cdot 46\text{H}_2\text{O}$ , a new mineral with a  
286 heteropolytungstate tri-lacunary Keggin anion. American Mineralogist, 99, 1045-1051.
- 287 Kampf, A.R., Hughes, J.M., Nash, B.P., and Marty, J. (2016) Vanarsite, packratite, morrisonite,  
288 and gatewayite: four new minerals containing the  $[\text{As}^{3+}\text{V}^{4+,5+}_{12}\text{As}^{5+}_6\text{O}_{51}]$  heteropolyanion, a  
289 novel polyoxometalate cluster. Canadian Mineralogist, 54, 145-162.
- 290 Kampf, A.R., Nash, B.P., Marty, J., Hughes, J.M., and Rose, T.P. (2017a) Hydropascoite,  
291  $\text{Ca}_3(\text{V}_{10}\text{O}_{28})\cdot 24\text{H}_2\text{O}$ , a new decavanadate mineral from the packrat mine, Mesa County,  
292 Colorado. Canadian Mineralogist, 55, 207-217.
- 293 Kampf, A.R., Hughes, J.M., Nash, B.P. and Marty, J. (2017b) Kegginite,  
294  $\text{Pb}_3\text{Ca}_3[\text{AsV}_{12}\text{O}_{40}(\text{VO})]\cdot 20\text{H}_2\text{O}$ , a new mineral with an  $\epsilon$ -isomer of the Keggin anion.  
295 American Mineralogist, 102, 461-465.
- 296 Kato, R., Kobayashi, A., and Sasaki, Y. (1982) The heteropolyvanadate of Phosphorus.  
297 Crystallographic and NMR Studies. Inorganic chemistry, 21, 240-246.
- 298 Katsoulis, D. (1998) A survey of applications of polyoxometalates. Chemistry of Materials, 98,  
299 359-387.
- 300 Mandarino, J.A. (2007) The Gladstone–Dale compatibility of minerals and its use in selecting  
301 mineral species for further study. Canadian Mineralogist, 45, 1307-1324.
- 302 Nyman, M., Maginn, E.J., Larentzos, J.P., Bonhomme, F.J., Parise, B., Welk, M.E., Bull, I. and  
303 Park, H. (2007) Experimental and theoretical methods to investigate extraframework species  
304 in a layered material of dodecaniobate anions. Inorganic Chemistry, 46, 2067–2079.

- 305 Pouchou, J.-L. and Pichoir, F. (1991) Quantitative analysis of homogeneous or stratified  
306 microvolumes applying the model "PAP." In: Heinrich, K.F.J. and Newbury, D.E. (eds)  
307 *Electron Probe Quantitation*. Plenum Press, New York, pp. 31–75.
- 308 Schindler, M. and Hawthorne, F.C. (2000) A bond-valence approach to the structure, chemistry,  
309 and paragenesis of hydroxyl-hydrated oxysalt minerals. I. Theory. Canadian Mineralogist,  
310 39, 1225-1242.
- 311 Schindler, M., Hawthorne, F.C., and Baur, W.H. (2000) Crystal chemical aspects of vanadium:  
312 Polyhedral geometries, characteristic bond valences, and polymerization of (VO<sub>n</sub>)  
313 polyhedral. Chemical Materials, 12(5), 1248-1259.
- 314 Shawe, D.R. (2011) Uranium-vanadium deposits of the Slick Rock district, Colorado. United  
315 States Geological Survey Professional Paper 576-F.
- 316 Sheldrick, G.M. (2015) Crystal Structure refinement with SHELX. Acta Crystallographica, C71,  
317 3–8.
- 318

319



320

321

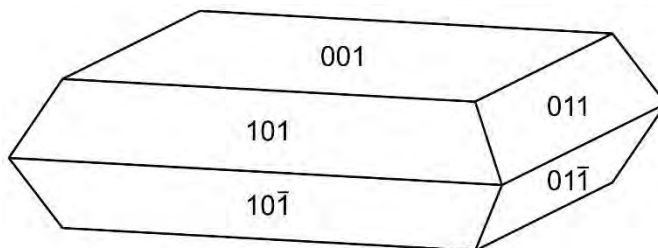
322 **FIGURE 1.** Bicapite with huemulite (orange) and minor gypsum; FOV 0.48 mm across.

323

324

325

326



327

328

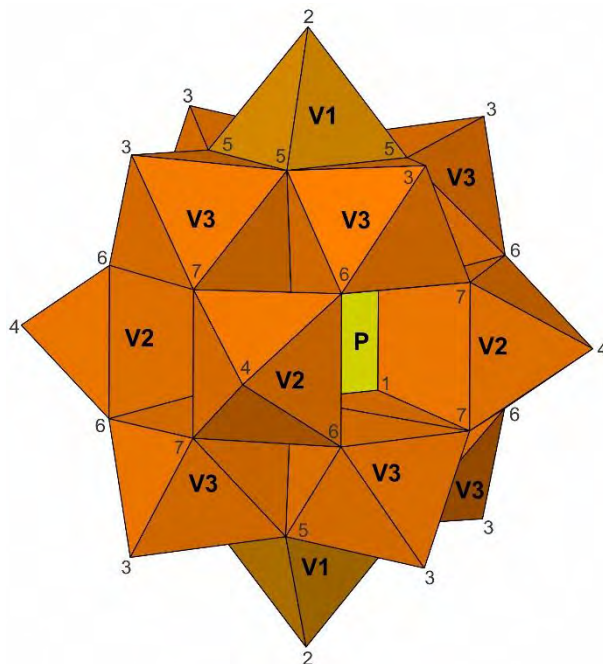
329

330 **FIGURE 2.** Crystal drawing of bicapite; clinographic projection.

331



332



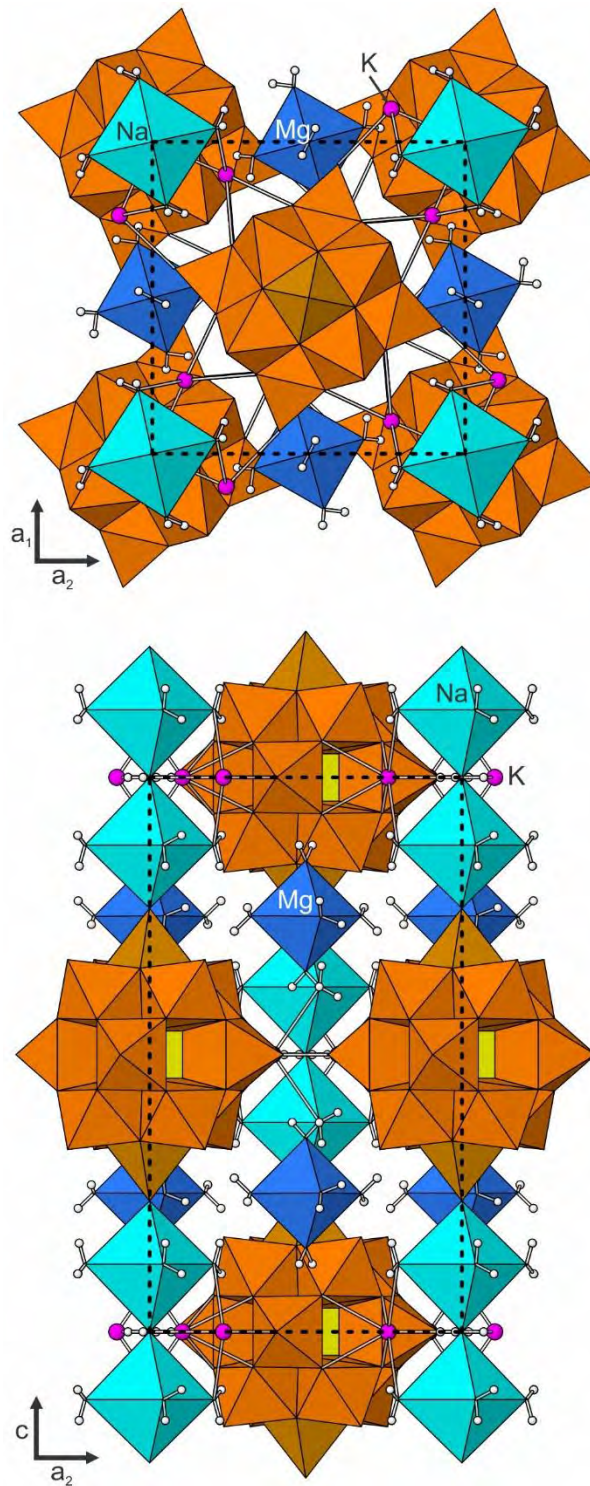
333

334

335 **FIGURE 3.** Bicapped Keggin anion that is the  $[\text{H}_2\text{PV}^{5+}_{12}\text{O}_{40}(\text{V}^{5+}\text{O})_2]^{7-}$  structural unit in  
336 bicapite. The O atom sites are numbered. The *c* axis is approximately vertical.

337

338



339

340

341

342

343

**FIGURE 4.** Structure of bicapite viewed down **c** (top) and down **a** (bottom). H atoms are shown as white balls. The unit cell is outlined with dashed lines.

344

345

346

**TABLE 1.** Analytical data (wt%) for bicapite

347

348

Const.	Mean	Range	S.D.	Standard	Norm.
K <sub>2</sub> O	3.49	3.32–3.65	0.17	sanidine	2.89
Na <sub>2</sub> O	4.16	3.68–4.52	0.35	albite	3.44
MgO	3.59	3.45–3.80	0.16	diopside	2.97
P <sub>2</sub> O <sub>5</sub>	4.35	4.15–4.49	0.15	apatite	3.60
V <sub>2</sub> O <sub>5</sub>	76.25	75.72–76.69	0.54	V metal	63.04
MoO <sub>3</sub>	0.61	0.42–0.77	0.18	Mo metal	0.50
H <sub>2</sub> O*					23.57
Total					100.01

349

350

351

352

353

354

355

356

357

358

\*Based upon the crystal structure with V + P + Mo = 15 and  
O = 67 apfu.

359

360

361

362  
 363  
 364  
 365

**TABLE 2.** Observed and calculated powder X-ray diffraction data ( $d$  in Å) for bicapite

$I_{\text{obs}}$	$d_{\text{obs}}$	$d_{\text{calc}}$	$I_{\text{calc}}$	$hkl$	$I_{\text{obs}}$	$d_{\text{obs}}$	$d_{\text{calc}}$	$I_{\text{calc}}$	$hkl$
100	10.14	{ 10.2999	16	0 0 2	11	2.583	{ 2.5779	7	4 2 0
		10.0602	84	1 0 1			2.5750	3	0 0 8
6	8.13	8.1519	7	1 1 0	4	2.505	{ 2.5151	1	4 0 4
5	5.897	5.8994	5	1 0 3			2.4994	2	1 3 6
		5.7643	1	2 0 0	5	2.314	2.3136	4	1 4 5
		5.1500	1	0 0 4			2.2914	1	4 3 1
10	5.037	{ 5.0301	4	2 0 2			2.2609	1	1 5 0
		5.0014	6	1 2 1			2.2074	1	4 0 6
10	4.348	4.3539	8	1 1 4	3	2.1778	{ 2.1858	1	5 0 3
8	4.142	4.1229	6	2 1 3			2.1769	1	2 2 8
7	3.810	{ 3.8405	3	2 0 4			2.1653	1	2 3 7
		3.7900	3	2 2 2	2	2.1234	2.1293	1	5 2 1
		3.7777	1	3 0 1			2.1032	1	3 1 8
2	3.439	3.4367	1	1 3 2	4	2.0805	{ 2.0920	1	2 1 9
7	3.357	3.3534	7	3 0 3			2.0702	1	5 1 4
4	3.220	3.2186	3	1 2 5	3	2.0317	{ 2.0438	1	2 5 3
6	3.170	{ 3.1641	1	1 1 6			2.0270	1	4 1 7
		3.1596	5	3 2 1			1.9665	1	3 0 9
29	2.978	2.9755	30	1 3 4			1.9214	1	6 0 0
		2.9497	1	2 0 6	5	1.8939	{ 1.8888	2	6 0 2
		2.8986	1	2 3 3			1.8873	3	1 6 1
4	2.882	{ 2.8821	2	4 0 0	3	1.8603	{ 1.8691	1	3 3 8
		2.8102	10	3 0 5			1.8612	1	3 2 9
11	2.809	2.7173	2	3 3 0	8	1.8199	{ 1.8228	2	2 6 0
3	2.706	2.6274	1	3 3 2			1.8218	4	4 2 8

366 Refined unit-cell parameters:  $a = 11.583(13)$ ,  $c = 20.68(2)$  Å,  $V = 2775(7)$  Å<sup>3</sup>.  
 367

368 **TABLE 3.** Data collection and structure refinement details for bicapite

369	Diffractometer	Rigaku R-Axis Rapid II
370	X-ray radiation / power	MoK $\alpha$ ( $\lambda = 0.71075 \text{ \AA}$ )/50 kV, 40 mA
371	Temperature	293(2) K
372	Empirical Formula	H <sub>42</sub> K <sub>1.49</sub> Mg <sub>1.89</sub> Na <sub>1.93</sub> O <sub>66.98</sub> P <sub>1</sub> V <sub>14</sub>
373	Space group	<i>I4/m</i>
374	Unit cell dimensions	$a = 11.5446(12) \text{ \AA}$
375		$c = 20.5460(14) \text{ \AA}$
376	<i>V</i>	2738.3(6) $\text{\AA}^3$
377	<i>Z</i>	2
378	Density (for above formula)	2.434 g cm <sup>-3</sup>
379	Absorption coefficient	2.594 mm <sup>-1</sup>
380	<i>F</i> (000)	1974.1
381	Crystal size	140 × 80 × 30 $\mu\text{m}$
382	$\theta$ range	3.19 to 24.98°
383	Index ranges	$-13 \leq h \leq 12, -13 \leq k \leq 13, -24 \leq l \leq 24$
384	Refls collected / unique	10217 / 1245; $R_{\text{int}} = 0.057$
385	Reflections with $I > 2\sigma I$	1008
386	Completeness to $\theta = 24.98^\circ$	99.4%
387	Max. and min. transmission	0.926 and 0.713
388	Refinement method	Full-matrix least-squares on $F^2$
389	Parameters / restraints	141 / 10
390	GoF	1.100
391	Final <i>R</i> indices [ $F_o > 4\sigma(F)$ ]	$R_1 = 0.0465, wR_2 = 0.1133$
392	<i>R</i> indices (all data)	$R_1 = 0.0578, wR_2 = 0.1214$
393	Largest diff. peak / hole	+0.54 / -0.60 e/ $\text{\AA}^3$
394	* $R_{\text{int}} = \Sigma F_o^2 - F_c^2(\text{mean}) /\Sigma[F_o^2]$ . GoF = $S = \{\Sigma[w(F_o^2 - F_c^2)^2]/(n-p)\}^{1/2}$ . $R_1 = \Sigma  F_o  -  F_c  /\Sigma F_o $ . $wR_2$	
395	= $\{\Sigma[w(F_o^2 - F_c^2)^2]/\Sigma[w(F_o^2)^2]\}^{1/2}$ ; $w = 1/[\sigma^2(F_o^2) + (aP)^2 + bP]$ where $a$ is 0.0578, $b$ is 13.824 and	
396	$P$ is $[2F_c^2 + \text{Max}(F_o^2, 0)]/3$ .	

397

398

399

**TABLE 4.** Atom coordinates and displacement parameters ( $\text{\AA}^2$ ) for bicapite

	<i>x/a</i>	<i>y/b</i>	<i>z/c</i>	$U_{eq}$	Occupancy		
400							
401	P	0	0	0.5	0.0201(7)	1	
402	V1	0	0	0.31386(8)	0.0295(4)	1	
403	V2	0.29689(10)	-0.05685(10)	0.5	0.0306(4)	1	
404	V3	0.18565(7)	0.12493(7)	0.38618(4)	0.0313(3)	1	
405	Mg	0.5	0	0.25	0.0305(13)	0.944(15)	
406	Na	0.5	0.5	0.62235(19)	0.0415(17)	0.966(17)	
407	K/O	0.3951(3)	0.2637(3)	0.5	0.0608(17)	K: 0.372(14); O: 0.628(14)	
408	OW	0.4463(12)	0.1529(14)	0.5841(8)	0.025(6)	0.184(11)	
409	O1	0.1059(5)	-0.0230(5)	0.4572(3)	0.0264(14)	0.5	
410	O2	0	0	0.2361(3)	0.0416(18)	1	
411	O3	0.2624(3)	0.1777(3)	0.32880(17)	0.0412(9)	1	
412	O4	0.4277(4)	-0.0938(4)	0.5	0.0469(14)	1	
413	O5	0.0299(3)	0.1487(3)	0.34411(19)	0.0393(9)	1	
414	O6	0.2960(5)	0.0526(3)	0.4346(2)	0.0711(15)	1	
415	O7	0.1688(3)	0.2447(5)	0.4368(2)	0.0792(18)	1	
416	OW1	0.5	0.500000	0.5	0.060(3)	1	
417	H1	0.52(2)	0.569(7)	0.5	0.071	1	
418	OW2	0.5	0	0.3506(3)	0.0447(13)	1	
419	H2	0.543(4)	-0.021(6)	0.378(2)	0.054	1	
420	OW3	0.4516(3)	0.1778(3)	0.2505(2)	0.0428(10)	1	
421	H3A	0.385(3)	0.186(5)	0.265(3)	0.051	1	
422	H3B	0.456(5)	0.229(4)	0.223(2)	0.051	1	
423	OW4	0.5446(5)	0.2936(5)	0.6219(3)	0.0746(15)	1	
424	H4A	0.602(5)	0.270(7)	0.605(3)	0.090	1	
425	H4B	0.550(7)	0.275(7)	0.6599(16)	0.090	1	
426		$U^{11}$	$U^{22}$	$U^{33}$	$U^{23}$	$U^{13}$	$U^{12}$
427	P	0.0213(10)	0.0213(10)	0.0176(16)	0	0	0
428	V1	0.0349(6)	0.0349(6)	0.0186(8)	0	0	0
429	V2	0.0254(6)	0.0316(7)	0.0349(7)	0	0	-0.0006(4)
430	V3	0.0329(5)	0.0386(5)	0.0223(5)	-0.0006(3)	0.0037(3)	-0.0078(3)
431	Mg	0.0341(16)	0.0341(16)	0.023(2)	0	0	0
432	Na	0.050(2)	0.050(2)	0.024(3)	0	0	0
433	K	0.047(2)	0.063(3)	0.073(3)	0	0	0.0022(16)
434	OW	0.012(9)	0.036(11)	0.027(10)	-0.006(7)	-0.009(7)	-0.005(6)
435	O1	0.032(3)	0.030(3)	0.018(3)	-0.003(3)	0.003(3)	0.002(3)
436	O2	0.052(3)	0.052(3)	0.020(4)	0	0	0
437	O3	0.039(2)	0.054(2)	0.031(2)	0.0046(17)	0.0069(16)	-0.0083(17)
438	O4	0.027(3)	0.038(3)	0.076(4)	0	0	-0.001(2)
439	O5	0.0282(18)	0.041(2)	0.049(2)	-0.0127(17)	-0.0020(16)	0.0022(14)
440	O6	0.116(4)	0.033(2)	0.064(3)	0.016(2)	-0.059(3)	-0.021(2)
441	O7	0.035(2)	0.130(4)	0.073(3)	-0.070(3)	-0.014(2)	0.025(2)
442	OW1	0.069(5)	0.069(5)	0.040(7)	0	0	0
443	OW2	0.046(3)	0.061(4)	0.028(3)	0	0	0.000(3)
444	OW3	0.040(2)	0.044(2)	0.044(2)	0.0035(18)	0.0128(18)	0.0039(17)
445	OW4	0.079(4)	0.059(3)	0.086(4)	0.001(3)	0.023(3)	0.015(3)
446							

447 **TABLE 5.** Selected bond distances (Å) and angles (°) in bicapite

448	P–O1 (×4)	1.529(6)	<b>V3–O3</b>	<b>1.596(3)</b>	Na–O2	2.338(8)
449			<b>V3–O7</b>	<b>1.742(4)</b>	Na–OW4 (×4)	2.438(5)
450	<b>V1–O2</b>	<b>1.597(7)</b>	V3–O6	1.818(4)	Na–OW1	2.514(4)
451	V1–O5 (×4)	1.858(3)	V3–O5	2.014(3)	<Na–O>	2.434
452	<V1–O>	1.858	V3–O5	2.031(3)		
453			V3–O1	2.388(6)	K–O4	2.833(6)
454	<b>V2–O4</b>	<b>1.569(5)</b>	<V3–O>	1.999	K–O7 (×2)	2.925(5)
455	V2–O6 (×2)	1.845(4)			K–OW1	2.985(4)
456	V2–O7 (×2)	1.928(4)	Mg–OW2 (×2)	2.068(5)	K–O6 (×2)	3.009(5)
457	V2–O1	2.405(6)	Mg–OW3 (×4)	2.128(4)	K–OW4 (×2)	3.061(6)
458	<V2–O>	1.990	<Mg–O>	2.116	<K–O>	2.976
459						
460	Hydrogen bonds					
461	<i>D–H</i> ··· <i>A</i>	<i>D–H</i>	<i>H</i> ··· <i>A</i>	<i>D</i> ··· <i>A</i>	$\angle D–H–A$	
462	OW1–H1···K(H <sub>2</sub> O)	0.84(3)	2.16(6)	2.985(4)	166(7)	
463	OW2–H2···O6	0.79(3)	2.22(3)	2.982(7)	162(6)	
464	OW3–H3a···O3	0.83(3)	1.93(3)	2.712(5)	157(5)	
465	OW3–H3b···O5	0.82(3)	1.98(3)	2.800(6)	178(6)	
466	OW4–H4a···O7	0.80(3)	2.28(3)	3.074(8)	169(8)	
467	OW4–H4b···OW3	0.81(3)	2.44(5)	3.131(8)	144(8)	

468 V–O vanadyl bonds (Schindler and Hawthorne 2000) in bold.

469

470 **TABLE 6.** Bond-valence sums for bicapite. Values are expressed in valence units\*

471

	K	Na	Mg	P	V1	V2	V3	H bonds		$\Sigma$
								Acc.	Don.	
O1				1.27 ( $\times 4 \downarrow$ )		0.21	0.22 ( $\times \frac{1}{2} \downarrow \rightarrow$ ) 0.20 ( $\times \frac{1}{2} \downarrow \rightarrow$ )			1.69
O2		0.22			1.68					1.90
O3							1.69	0.22		1.91
O4	0.14 ( $\times 0.37 \rightarrow$ )					1.81				1.86
O5					0.86 ( $\times 4 \downarrow$ )		0.57 0.55	0.18		2.16
O6	0.09 ( $\times 2 \downarrow$ ) ( $\times 0.37 \rightarrow$ )					0.89 ( $\times 2 \downarrow$ )	0.95	0.13		2.00
O7	0.11 ( $\times 2 \downarrow$ ) ( $\times 0.37 \rightarrow$ )					0.72 ( $\times 2 \downarrow$ )	1.16	0.12		2.04
OW1	0.10 ( $\times 4 \times 0.37 \rightarrow$ )	0.14 ( $\times 2 \rightarrow$ )							-0.11 -0.11	0.06
OW2			0.35 ( $\times 2 \downarrow$ )						-0.13 -0.13	0.09
OW3			0.31 ( $\times 4 \downarrow$ )					0.11	-0.22 -0.18	0.01
OW4	0.08 ( $\times 2 \downarrow$ ) ( $\times 0.37 \rightarrow$ )	0.17 ( $\times 4 \downarrow$ )							-0.11	0.09
$\Sigma$	0.80	1.04	1.94	5.08	5.12	5.23	5.13			

472 \*Bond valence parameters are from Gagné and Hawthorne (2015). Hydrogen-bond strengths  
 473 based on O–O bond lengths from Ferraris and Ivaldi (1988).